

Cellular Uptake and Metabolism of DNA Frayed Wires[†]

M. F. Yanze, W.-S. Lee, K. Poon, M. Piquette-Miller, and R. B. Macgregor, Jr.*

Department of Pharmaceutical Sciences, Leslie Dan Faculty of Pharmacy, University of Toronto, 19 Russell Street, Toronto, Ontario M5S 2S2, Canada

Received February 21, 2003; Revised Manuscript Received August 8, 2003

ABSTRACT: DNA frayed wires are a novel, multistranded form of DNA that arises from interactions between single-stranded oligodeoxyribonucleotides with the general sequence $d(N_xG_y)$ or $d(G_yN_x)$, where $y > 10$ and $x > 5$. Frayed wires exhibit greater stability with respect to thermal and chemical denaturation than single- or double-stranded DNA molecules and, thus, may have potential usefulness for DNA drug delivery. However, the stability and uptake of frayed wires have not been investigated in biological systems. Our objective was to examine the cellular uptake and stability of frayed wires in cultured hepatic cells. In these studies, the parent oligonucleotide $d(A_{15}G_{15})$ was used to form DNA frayed wires (DNA_{FW}) while a random 30-mer oligonucleotide was used as the control nonaggregated DNA (DNA_{SS}). Uptake and metabolism studies of DNA_{FW} were performed in cultured human hepatoma, HepG2 cells and compared to DNA_{SS}. Our results indicate that DNA_{FW} are not cytotoxic and that their intracellular uptake in HepG2 cells is 2–3.5-fold greater than that of DNA_{SS} within the first 2 h ($p < 0.05$). Similarly, nuclear localization of DNA_{FW} is 10–13-fold higher than that of DNA_{SS} ($p < 0.05$). As both internalized and extracellular DNA_{FW} appear to be more stable in vitro than DNA_{SS}, the enhanced uptake may be due to either increased stability or enhanced intracellular transport. These studies also indicate that uptake of DNA_{FW} likely occurs via active processes such as receptor-mediated endocytosis similar to mechanisms which have been proposed for DNA_{SS}. The internalization pathways of DNA_{FW} may differ somewhat from that of DNA_{SS} insofar as chloroquine does not appear to alter DNA_{FW} uptake and degradation, as is the case with DNA_{SS}.

A major obstacle in gene therapy is the transport of intact DNA to target sites. Clinical implementation of oligonucleotide therapy requires overcoming two major obstacles: free single-stranded DNA displays poor cellular uptake, and it is extremely labile in a biological environment. The uptake is unfavorable because of the relatively large size and electrostatic charge of these molecules while the stability of free DNA in vivo is limited due to the presence of nucleases that rapidly hydrolyze phosphodiester bonds. Much effort has been directed at exploring viral and nonviral delivery systems to circumvent these barriers. Despite the effective transfection property of viral vectors, potentially serious side effects have decreased the enthusiasm and stimulated the development of the nonviral vectors (1–3).

Among the methods attempted to enhance the uptake, stability, and efficacy of oligonucleotides are endocytic delivery such as liposome-based uptake, oligonucleotide–lipid conjugates, poly(L-lysine)–oligonucleotide conjugates, nanoparticle-mediated uptake, receptor-based delivery, and dendrimer-based carrier systems. Invasive, nonendocytic delivery methods include electroporation, microinjection, and permeabilization. Noninvasive nonendocytic delivery techniques that have been tested include antennapedia homeodomain peptide, tat peptides, amphipathic model peptides, and signal peptides (4, 5).

DNA frayed wires (DNA_{FW})¹ are polydisperse aggregates of oligonucleotides arising from the self-association of “parent” oligonucleotides with runs of several consecutive guanines at the 3′ or 5′ end. In general, the sequence of parent oligonucleotides that form frayed wires is $d(N_xG_y)$ or $d(G_yN_x)$, where $x > 5$, $y > 10$, and N is any base (6–8). DNA_{FW} consist of aggregates of integer numbers of the parent oligonucleotide; species consisting of 2, 3, 4, 5, etc. associated oligonucleotides are observed as a ladder pattern in native and denaturing gel electrophoresis (10, 11). Structurally, DNA_{FW} behave as though they consist of two structurally and thermodynamically independent domains: a stem that is composed of noncovalent interactions between the guanine residues and arms made up of the non-guanine residues (9, 12–15). The stem is stable toward chemical and thermal denaturation, and it is resistant to enzymatic degradation (12). The arms also exhibit enhanced stability with respect to enzymatic degradation. They can also form standard double- and triple-stranded structures presumably through Watson–Crick base-pairing interactions (16). We were interested in evaluating the cellular uptake and stability of DNA_{FW} in vitro prior to initiating in vivo studies. Hence we examined the transport kinetics of DNA_{FW} in the human hepatoma HepG2 continuous cell line and compared it to

[†] This work was supported by a contract to M.P.-M. and R.B.M. from Glaxo SmithKline. F.M.Y. was supported by Helen Rosenstadt Funds and a postdoctoral fellowship from Rx&D/CIHR.

* To whom correspondence should be addressed. E-mail: rob.macgregor@utoronto.ca.

¹ Abbreviations: DNA_{FW}, DNA frayed wires; DNA_{SS}, single-stranded DNA; FBS, fetal bovine serum; PBS, phosphate-buffered saline; α MEM, α minimum essential medium; MTT, 3-(dimethylthiazol-2-yl)-2,5-diphenyl-2H-tetrazolium bromide; 5′-FAM, fluorescein 5′-phosphoramidite; HEX, hexachlorofluorescein 5′-phosphoramidite; cpm, counts per minute.

that of conventionally stranded DNA (DNA_{SS}). A second objective was to determine whether DNA_{FW} uptake occurs through active uptake processes such as those that have been proposed for conventionally stranded DNA (1–5, 17–19). Specifically, we addressed the following questions: (1) Is DNA_{FW} cytotoxic? (2) Is the cellular uptake of DNA_{FW} concentration and temperature dependent? (3) Is the uptake of DNA_{FW} energy dependent? (4) Are receptor-mediated endocytosis pathways involved in DNA_{FW} internalization? (5) How does the in vitro stability of DNA_{FW} compare to that of conventionally stranded DNA?

MATERIALS AND METHODS

DNA Frayed Wires. The labeling and synthesis of DNA_{FW} using the parent oligonucleotide sequence (A₁₅G₁₅) were carried out according to published protocols (6, 15). A random oligonucleotide sequence (5'-ACT TAG GCA CCA AGT ACT CTT TAC GTA TAA-3') was used as control single-stranded DNA (DNA_{SS}). Unlabeled oligonucleotides and fluorescein 5'-phosphoramidite labeled oligonucleotide were purchased from the Centre for Applied Genomics (Hospital for Sick Children, Toronto, Canada). T4 polynucleotide kinase was purchased from MBI Fermentas (Burlington, Canada) and [γ -³²P]ATP from Amersham Biosciences (Quebec, Canada). Labeled DNA_{FW} and labeled control oligodeoxyribonucleotides were diluted to the desired concentration with PBS (phosphate-buffered saline, pH 7.22), and the samples were stored at -20 °C until needed. The specific activity of labeled compounds ranged from 9×10^6 to 11×10^6 cpm/ μ g.

Cell Culture. Cell transport and metabolism studies were carried out using HepG2 cells, a human hepatoma cell line obtained from the American Type Tissue Culture Collection. The cells were maintained via serial culture in α MEM (α minimum essential medium; GibcoBRL Life Technologies) supplemented with 10% FBS (fetal bovine serum; Sigma Life Sciences) and 1% penicillin-streptomycin (GibcoBRL Life Technologies). The cells were grown to confluency in six-well microwell plates (Corning Inc.) in an incubator with conditions set to 37 °C, 5% CO₂, and 95% O₂. Cell protein was quantified using a colorimetric Bio-Rad protein assay (Bio-Rad, Inc.). Cell viability after each treatment was assessed using Trypan blue exclusion assay.

Cytotoxicity Assay. HepG2 cell suspensions of 7.5×10^5 cells/mL were plated at 100 μ L/well in 96-microwell culture plates. Cells were allowed to adhere overnight in an incubator. After a 24 h incubation of the cells with several concentrations of DNA_{FW} or DNA_{SS} (0–100 μ M), the MTT [3-(dimethylthiazol-2-yl)-2,5-diphenyl-2H-tetrazolium bromide] assay was carried out according to the manufacturer's protocol (Sigma Life Sciences) (21, 22). To determine the activity of mitochondrial dehydrogenase, the optical density (OD) was measured with a Spectra Max 384 Plus UV-visible plate reader (Spectra Max, Sunnyvale, CA). All values were determined four times.

Transport and Metabolism Studies. For the cell uptake studies, cultured HepG2 cells were incubated for various time periods at 37 °C with radiolabeled DNA_{FW} or DNA_{SS}; the concentration and temperature were also varied. After incubation the cells were washed three times with 500 μ L of ice-cold acetate buffer, pH 3, and lysed with an aqueous

solution of 0.5% Triton X-100. The radioactivity of aliquots of cell lysates was then quantified by scintillation counting (Beckman Instruments, Fullerton, Canada). The zero point corresponds to cells that were only allowed a very brief (<1 min) contact with DNA. For inhibition studies, inhibitors were added to the cell media 15 min prior to the addition of labeled DNA_{FW} or DNA_{SS} (0.4 μ M), and the uptake at 1 h was examined. We examined the following compounds: sodium azide (0–50 mM) and 2-deoxy-D-glucose (0–50 mM), which are metabolic inhibitors; heparin (0–20 units/mL), which is an inhibitor of receptor-mediated endocytosis; and chloroquine (0–100 μ M), a lysosomotropic agent which inhibits endosome/lysosome DNA degradation; and competitive inhibition with unlabeled DNA_{FW} or DNA_{SS}. The extent of degradation or metabolism of DNA_{FW} and DNA_{SS} incubated for up to 24 h with HepG2 cells was assessed in both extracellular and intracellular samples by electrophoresis on denaturing polyacrylamide gels (10% acrylamide, 7 M urea, 50 °C, 55 W, 45 min). Lanes containing ³²P-labeled DNA_{FW} and DNA_{SS} reaction mixes and free [γ -³²P]ATP were included as controls. The electrophoresis gels were dried, and the bands were visualized on an Ambis Model 4000 radioanalytic imaging system (Scanalytics, Inc., Billerica, MA).

Nuclear Localization. Nuclear localization and quantification of DNA_{FW} were assessed via centrifugation of fluorescently labeled parent oligonucleotides. Quantification of oligonucleotides labeled with 5'-FAM (fluorescein 5'-phosphoramidite) located within the nuclear fraction was performed by centrifugation in a sucrose density gradient using a Beckman Model L5-75 ultracentrifuge (Beckman, Inc., Mississauga, Ontario, Canada) (22). Confluent cells in 175 cm² culture flasks were incubated for 1 h with a 2 μ M solution of fluorescein-labeled DNA_{FW}. Then cells were washed three times with 10 mL of ice-cold acetate buffer, pH 3, trypsinized, and homogenized with a Dounce homogenizer. The homogenate was vortexed with 8 mL of 60% sucrose in TKM (50 mM Tris-HCl, pH 7.6, 25 mM KCl, 5 mM MgCl₂) and spun at 130000g min for 30 min at 5 °C. The pellet was washed, resuspended in 1 mL of PBS, vortexed with 9 mL of 60% sucrose in TKM, and spun at 120000g min for 30 min at 5 °C. This second pellet was washed and resuspended in 1 mL of PBS, aliquots were plated, and the fluorescence intensity was measured in a Spectra Max Gemini XS fluorescence plate reader (Spectra Max, Sunnyvale, CA). The experiments were run in duplicate. Nuclear localization and quantification of DNA_{SS} were also assessed. The fluorescent background of the cells was measured in nuclear fractions incubated with unlabeled DNA_{FW} or DNA_{SS}, respectively.

Confocal Microscopy. HepG2 cells were grown and incubated with a mix of 0.4 μ M HEX-DNA_{FW} and 5'-FAM-DNA_{SS} in 35 mm culture dishes. After incubation for 10 min, the cells were fixed by washing three times with 4% paraformaldehyde for 10 min at room temperature, washed three times with PBS, and mounted in a glycerin/PBS mixture (50:50). Colocalization was then investigated using an LSC 510 Meta confocal scanning laser microscope with upright Axioplan 2 imaging, equipped with an oil immersion 40 \times objective (Zeiss).

Statistics. The results are presented as averages \pm standard deviation of each experiment. For the uptake experiments,

the units are μg of DNA $(\mu\text{g}/\mu\text{L cell protein})^{-1} \text{ min}^{-1}$ or the percent uptake of DNA over the input amount. Inhibition and energy dependence studies are presented as the percent inhibition relative to untreated cells. The kinetic parameters, K_m and V_{\max} , were obtained by fitting the data to the Michaelis–Menten equation using SigmaPlot 2000. Statistics were performed with Excel 2000 using Student's *t*-test with $\alpha = 0.05$ or analysis of variance (ANOVA) according to the case.

RESULTS

In Vitro Toxicity of DNA Frayed Wires. Before undertaking the studies of the transport and metabolism of DNA_{FW}, we investigated their cytotoxicity by examining the effect of graded concentrations of DNA_{FW} and DNA_{SS} on the activity of mitochondrial dehydrogenase. Our results show that the activity of this enzyme in untreated cells and in cells treated with DNA_{FW} is the same after 24 h incubation [$f = 1.57 < f_{0.05}(6, 21) = 2.7$, $p = 0.21$], implying that DNA_{FW} is not toxic for the HepG2 cells (data not shown). We reached the same conclusion with DNA_{SS} [$f = 2.45 < f_{0.05}(6, 21) = 2.7$, $p = 0.06$]. This conclusion is consistent with previous results for DNA_{SS} (23).

Impact of Incubation Time on DNA Frayed Wire Uptake. The study of the time dependence of DNA_{FW} uptake shows that it increases from an initial value of $0.105 \pm 0.017 \mu\text{g}$ of DNA_{FW} $(\mu\text{g of cell protein})^{-1} \mu\text{L}^{-1}$ to a steady-state value of $0.300 \pm 0.053 \mu\text{g}$ of DNA_{FW} $(\mu\text{g of cell protein})^{-1} \mu\text{L}^{-1}$ at 30 min. Incubations as long as 120 min did not lead to statistically significant changes in this value. These observations suggest that the DNA_{FW} that accumulated in the cells remained intact during the 2 h experiment. DNA_{SS} uptake increases from an initial value of $0.052 \pm 0.01 \mu\text{g}$ of DNA_{SS} $(\mu\text{g of cell protein})^{-1} \mu\text{L}^{-1}$ to a maximum of $0.130 \pm 0.012 \mu\text{g}$ of DNA_{SS} $(\mu\text{g of cell protein})^{-1} \mu\text{L}^{-1}$ after 10 min. After 15 min, it decreased to the steady-state value of $0.086 \pm 0.012 \mu\text{g}$ of DNA_{SS} $(\mu\text{g of cell protein})^{-1} \mu\text{L}^{-1}$. The rate of uptake remained constant at this level for incubations as long as 120 min (longer incubations were not investigated). The decrease in the accumulation of DNA_{SS} may be explained by its instability in the cytosol. In addition to the enhanced stability of DNA_{FW} in the HepG2 cells, in all cases, uptake is always 2–3.5-fold greater than that of DNA_{SS} ($p < 0.05$).

Concentration Dependence of DNA Frayed Wire Uptake. Figure 1 shows that the uptake of DNA_{FW} into HepG2 cells becomes saturated at high concentrations. Saturation is indicative of a mechanism involving an active process and is consistent with active uptake processes that have been reported for conventionally stranded DNA (17, 18, 24–26). We fit the data to the Michaelis–Menten equation assuming that a simple bimolecular reaction underlies the uptake. The average V_{\max} value obtained from fitting the data to the Michaelis–Menten equation is 3-fold higher for DNA_{FW} [$0.08 \pm 0.02 \mu\text{g}$ of DNA_{FW} $(\mu\text{g of cell protein})^{-1} \mu\text{L}^{-1} \text{ min}^{-1}$] than for DNA_{SS} [$0.03 \pm 0.006 \mu\text{g}$ of DNA_{SS} $(\mu\text{g of cell protein})^{-1} \mu\text{L}^{-1} \text{ min}^{-1}$]. This parameter is indicative of the capacity of the transport mechanism for the two types of DNA. The relative affinity, as reflected in the average K_M value, was $0.60 \pm 0.27 \mu\text{M}$ for DNA_{FW} and $0.37 \pm 0.23 \mu\text{M}$ for DNA_{SS}. Thus, our data show that there are differences

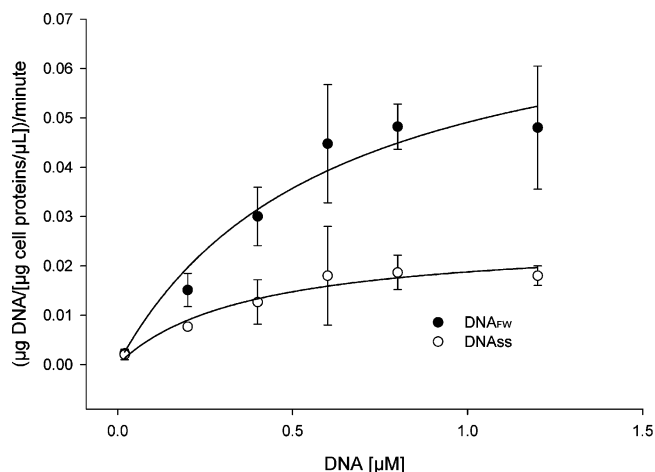


FIGURE 1: Concentration dependence of DNA_{FW} and DNA_{SS} uptake. The smooth lines are fits of the data to the Michaelis–Menten equation. The parameters of the fit yielded values of V_{\max} and K_m equal to $0.08 \pm 0.02 \mu\text{g}$ of DNA_{FW} $(\mu\text{g of cell protein})^{-1} \mu\text{L}^{-1} \text{ min}^{-1}$ and $0.60 \pm 0.27 \mu\text{M}$ for DNA_{FW}. For DNA_{SS} these two parameters equal $0.03 \pm 0.006 \mu\text{g}$ and $0.37 \pm 0.23 \mu\text{M}$, respectively. Error bars represent standard deviations.

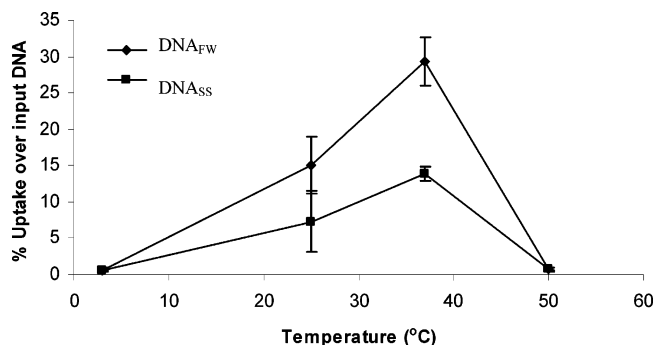


FIGURE 2: Temperature dependence of DNA_{FW} uptake. After equilibration at a given temperature (3, 25, 37, and 50 °C) cells were incubated for 1 h with $0.4 \mu\text{M}$ DNA_{FW} or DNA_{SS} according to the experiment. Error bars represent standard deviations.

in the capacity and relative affinity in the uptake pathway for these alternately stranded DNA species. Within error, the ratio of K_M/V_{\max} has the same value for DNA_{FW} and DNA_{SS}, suggesting that similar uptake mechanisms exist for these two forms of DNA. It is evident that the actual reaction mechanism leading to uptake of either of these two forms of DNA will involve more than the single bimolecular step we have assumed. However, in the absence of a more complete study of the mechanism of uptake, these kinetics parameters provide a basis for quantitative comparison of the two forms.

Temperature Dependence of DNA_{FW} Uptake. The dependence of the uptake on temperature (Figure 2) is similar for DNA_{FW} and DNA_{SS} although the uptake of DNA_{FW} at 25 and 37 °C is twice that of DNA_{SS} ($p < 0.05$). Uptake increases with temperature between 0 and 37 °C and decreases from 37 to 50 °C; this is also consistent with the involvement of active transport processes (1, 27–29). The rate of protein and enzyme-dependent processes commonly increases with temperature within the range of 0–37 °C (3, 30).

Energy Dependence of DNA_{FW} Uptake. ATP depletion by treatment of cells with sodium azide resulted in a concentration-dependent inhibition of DNA_{FW} uptake into HepG2 cells

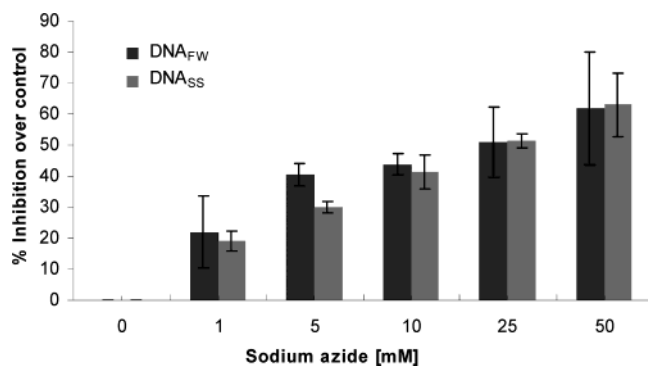


FIGURE 3: Energy dependence of DNA_{FW} uptake. Sodium azide was added 15 min prior to a 1 h incubation with 0.4 μ M DNA_{FW} or 0.4 μ M DNA_{SS}. Cell viability after treatment was assessed with Trypan blue exclusion assay. Error bars represent standard deviations. At the control point, 0, the uptake is not affected relative to the treated cells.

(Figure 3). Uptake was 62% inhibited after the cells were exposed to 50 mM sodium azide. Energy depletion in HepG2 cells by addition of the glucose inhibitor, 50 mM 2-deoxy-D-glucose, also led to a significant reduction ($16 \pm 5\%$) in the uptake of DNA_{FW}. Synergic inhibition ($39 \pm 1\%$) was observed upon incubation with 50 mM 2-deoxy-D-glucose and 1 mM sodium azide. Similarly, the transport of DNA_{SS} was also significantly reduced in cells that were treated with sodium azide or 2-deoxy-D-glucose (Figure 3). Inhibition of uptake after ATP or energy depletion is also consistent with the involvement of active transport processes in the uptake of DNA_{FW} and DNA_{SS}. Previous studies with these metabolic inhibitors have reported similar inhibition of cellular uptake of conventionally stranded oligonucleotides (17, 31–33).

Competitive Inhibition of DNA_{FW} Uptake. Addition of unlabeled DNA_{FW} or unlabeled DNA_{SS} resulted in a significant inhibition of DNA_{FW} uptake into HepG2 cells (Figure 4A). Addition of a solution containing 5–10 μ M unlabeled DNA_{FW} inhibited uptake by 50–65% whereas the same concentration of unlabeled DNA_{SS} resulted in a 29–57% inhibition. Similarly, the uptake of ³²P-labeled DNA_{SS} by these cells was inhibited in a concentration-dependent manner by unlabeled DNA_{SS} or DNA_{FW} (Figure 4B). In this case, addition of DNA_{SS} did not cause a greater inhibition than DNA_{FW} insofar as addition of solutions containing 5–10 μ M either unlabeled DNA species resulted in a 40–55% inhibition. This indicates that both the frayed wire structures and conventionally stranded DNA likely compete for similar binding sites to transporters involved in their uptake.

Cellular uptake of DNA_{SS} is generally thought to occur through receptor-mediated endocytosis (RME). The fact that unlabeled DNA_{FW} competes with DNA_{SS} uptake and unlabeled DNA_{SS} with DNA_{FW} uptake indicates that both species could compete for the same receptor-mediated pathway. Furthermore, the fact that the inhibition of DNA_{FW} uptake is greater after the addition of DNA_{FW} than after the addition of DNA_{SS} suggests that there may be a difference in the affinity or additional pathways for DNA_{FW} cellular uptake.

The heparin inhibition studies provided further evidence for the involvement of receptor-mediated endocytosis (RME) (Figure 4C). It has been reported that the receptor involved in the RME uptake of oligonucleotides possesses a heparin-binding protein (3, 34–37). Heparin, a specific inhibitor for this endocytosis pathway, inhibits DNA_{FW} and DNA_{SS} uptake

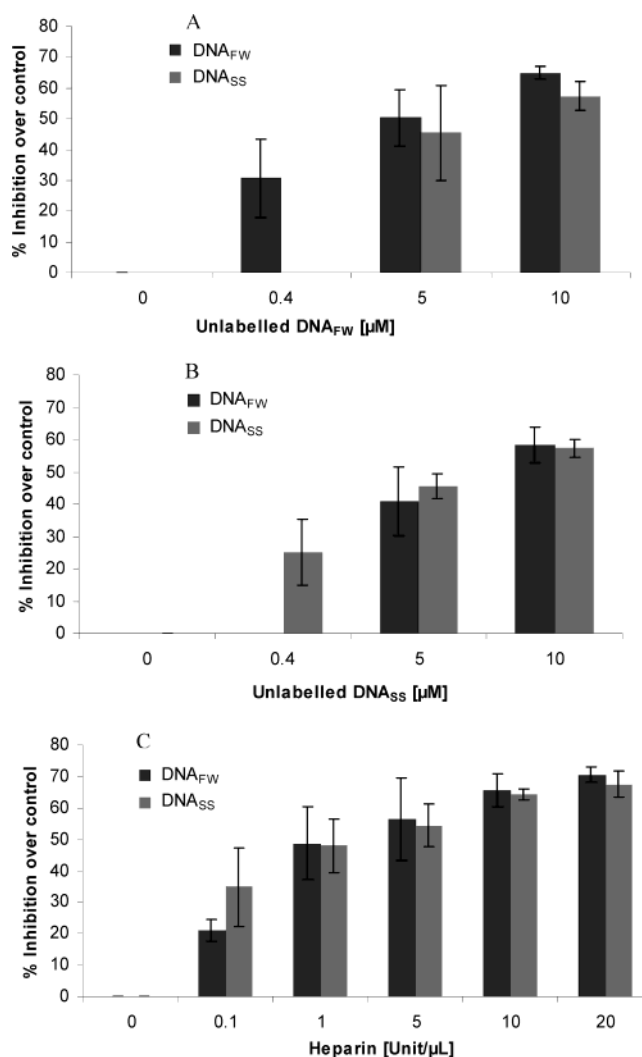


FIGURE 4: (A) Competitive inhibition of DNA_{FW} uptake. Unlabeled DNA_{FW} (0.4, 5, and 10 μ M) and unlabeled DNA_{SS} (5 and 10 μ M) competing with the uptake of labeled DNA_{FW}. (B) Competitive inhibition of DNA_{SS} uptake. Unlabeled DNA_{SS} (0.4, 5, and 10 μ M) and unlabeled DNA_{FW} (5 and 10 μ M) competing with the uptake of DNA_{SS}. (C) Inhibition of the uptake of DNA_{FW} and DNA_{SS} with heparin. The competitive inhibitors were added 15 min prior to the 1 h incubation with 0.4 μ M labeled DNA_{FW} or DNA_{SS}, respectively. Error bars represent standard deviations. At the control point, 0, the uptake is not affected relative to the treated cells.

in a concentration-dependent manner. Hence it is likely that the heparin-binding protein associated RME is involved in the uptake of both DNA_{FW} and DNA_{SS}. However, other receptor-mediated endocytosis pathways have been reported such as the DNA receptor protein, the nucleic acid binding receptor-1, heparin-binding Mac1, nucleolin-like proteins, and porin-like proteins (18, 19, 38–45). As complete inhibition could not be achieved by addition of heparin alone, it is plausible that one or more of these other RME proteins may also be involved in DNA_{FW} uptake.

Impact of Chloroquine on DNA_{FW} Internalization. Chloroquine enhances plasmid DNA uptake into cells through the inhibition of DNA degradation in endosomes (32, 33, 46–51). This lysosomotropic agent acts by raising endolysosomal pH, thereby creating a suboptimal biological pH environment for the enzymatic degradation of DNA. As previously reported, addition of chloroquine resulted in a

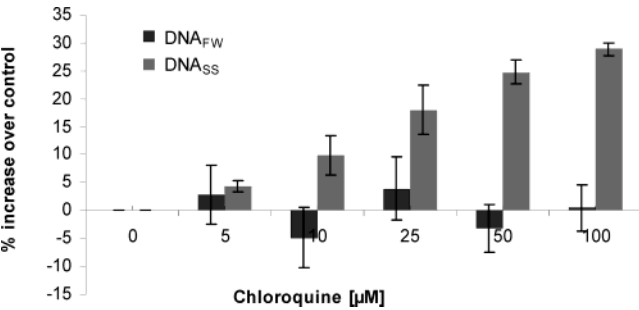


FIGURE 5: Impact of chloroquine on DNA_{FW} internalization. Chloroquine was added 15 min prior to a 1 h incubation with 0.4 μM labeled DNA_{FW} or 0.4 μM labeled DNA_{SS}. Error bars represent standard deviations. At the control point, 0, the uptake is not affected relative to the treated cells.

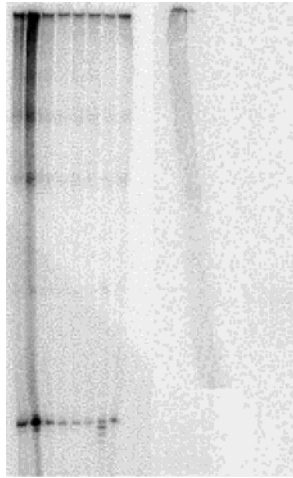


FIGURE 6: Stability of DNA_{FW} in HepG2 cells. From left to right: lanes 1 and 2 are control DNA_{FW} that had not been incubated with HepG2 cells; lanes 3–5 are extracellular reaction mixtures incubated for 1, 12, and 24 h, respectively, with HepG2 cells; lanes 6–8 are cell lysates incubated for 1, 12, and 24 h, respectively, with HepG2 cells; lane 9 is control DNA_{SS}. In all of the other lanes comparable to DNA_{FW} lanes, DNA_{SS} are completely degraded.

Table 1: Nuclear Localization of DNA_{FW} vs DNA_{SS}

	DNA _{FW}	DNA _{SS}	DNA _{FW} /DNA _{SS}
cell uptake			
% of overall input	34 ± 4	9 ± 1	4-fold
nuclear localization			
% of internalized DNA localized in nucleus	71 ± 2	27 ± 2	3-fold
% of total DNA localized in nucleus	24 ± 2	2.5 ± 0	10-fold

significant increase the intracellular uptake of DNA_{SS} in a concentration-dependent manner (Figure 5). This phenomenon is generally believed to result from RME-mediated internalization of DNA_{SS} into endosomes with a subsequent degradation by endosomal enzymes that are inhibited by chloroquine. However, exposure of the cells to solutions containing up to 100 μM chloroquine did not result in any meaningful changes in the intracellular uptake of DNA_{FW}.

Nuclear Localization and Quantification of DNA_{FW}. The results of these experiments (Table 1) carried out with fluorescently labeled DNA confirmed that DNA_{FW} uptake is greater than that of DNA_{SS} (34.2 ± 3.9% vs 9.3 ± 1.3, $p < 0.05$). The fluorescence intensity of the nuclear fraction showed that 71 ± 1.7% of DNA_{FW} cell uptake is localized

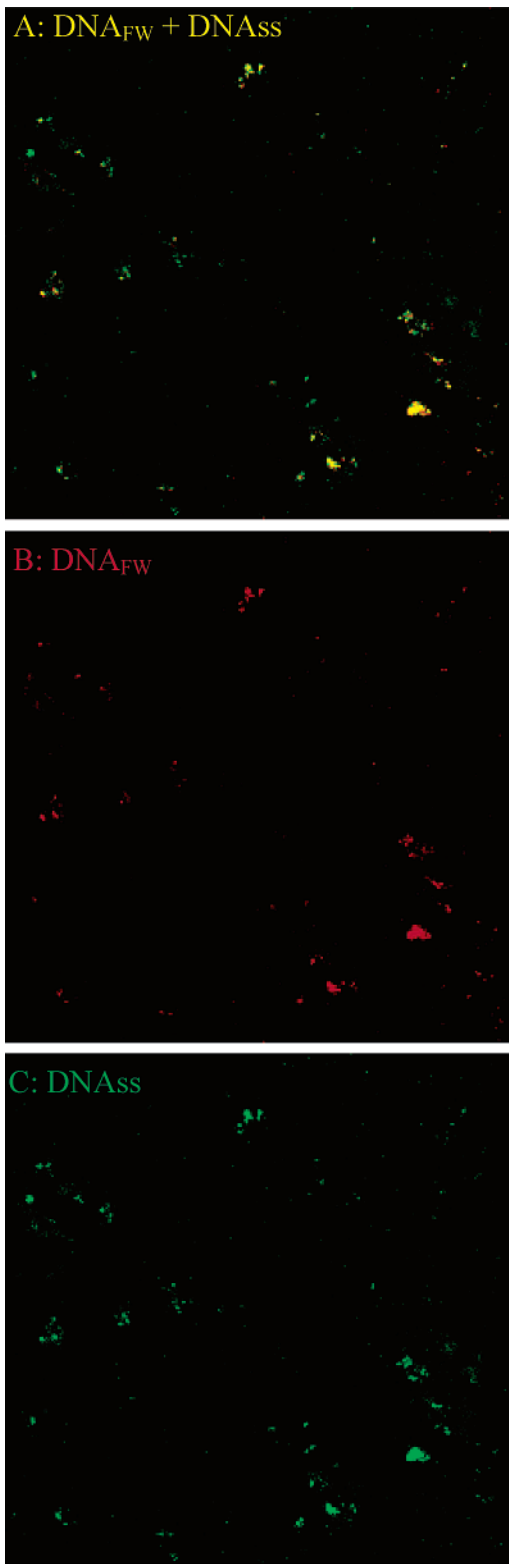


FIGURE 7: Colocalization of DNA_{FW} and DNA_{SS} in HepG2 cells. Cells were incubated for 10 min with a 0.4 μM mix of HEX–DNA_{FW} (red signal) and 5′-FAM–DNA_{SS} (green signal). The yellow, yellowish, and greenish signals shown in panel A demonstrate the colocalization of DNA_{FW} and DNA_{SS} in HepG2 cells. The split of panel A shows DNA_{FW} localization (panel B), and DNA_{SS} localization (panel C). The almost total disappearance of the red signal in panel A is consistent with the total colocalization.

in the nucleus, i.e., 24.3 ± 2.2% of the overall input. In contrast, only 26.7 ± 2% of the uptake of DNA_{SS} located in the nucleus; this represents 2.5 ± 0.2% of the overall input.

The concentration of DNA_{FW} in the nucleus is more than 10-fold higher than that of DNA_{SS}; presumably this may be due, in part, to the greater stability of DNA_{FW} in the cell.

Stability of DNA_{FW} in HepG2 Cells. As depicted in Figure 6, autoradiograms of internalized DNA_{FW} from HepG2 cell lysates demonstrated distinctive banding patterns similar to those of control DNA_{FW} preparations that had not been exposed to cells. Furthermore, we did not detect substantial degradation of the DNA_{FW} after up to 24 h of incubation with HepG2 cells, suggesting that minimal metabolism of DNA_{FW} occurs. Autoradiograms of DNA_{SS} incubated with HepG2 cells demonstrated almost complete degradation after 1 h of exposure to the cells (DNA bands migrated with free [³²P]ATP). These results underscore the greater stability of DNA_{FW} relative to other more standard DNA structures.

DISCUSSION

We have demonstrated that DNA_{FW} are not cytotoxic and that they are taken up into cells by a saturable, temperature-dependent, and inhibitable mechanism; this is suggestive of an active transport process. In particular, our results suggest that uptake of DNA_{FW} occurs through a receptor-mediated endocytosis pathway similar to the pathway that has been proposed for conventionally stranded DNA. These studies have demonstrated that, relative to conventional single-stranded DNA, DNA_{FW} display enhanced stability as well as increased intracellular and intranuclear uptake.

There are two alternative hypotheses that could account for these observations: The first possibility stems from the greater resistance of DNA_{FW} to enzymatic degradation by nucleases. Previous *in vitro* studies have shown that DNA_{FW} exhibit greater stability than DNA_{SS} toward hydrolysis by DNase I, mung bean nuclease, S1 nuclease, and Exo III (6, 12, 16). If one can extrapolate these results to the hydrolytic activity of endosomal enzymes toward DNA_{FW}, then chloroquine would not be expected to affect the uptake and stability of DNA_{FW} to the same extent that would be seen with other DNA structures. This hypothesis has been verified by the colocalization imaging with the laser scanning confocal microscope depicted in Figure 7. A second explanation for the results would be differences in the uptake and internalization patterns (3, 52–54) or the same uptake but different internalization (18, 50) of DNA_{FW} relative to DNA_{SS}. This hypothesis seems less plausible because similar uptake, inhibition, and localization profiles were seen with DNA_{SS} and DNA_{FW}, suggesting comparable transport mechanisms. However, DNA_{FW} transport into cells may, in part, occur via additional uptake processes.

In conclusion, the finding that DNA_{FW} display improved stability and uptake in a biological system underscores the need to perform further studies to optimize its use as a DNA delivery device.

REFERENCES

- Vlassov, V. V., Balakireva, L. A., and Yakubov, L. A. (1994) *Biochim. Biophys. Acta* 1197, 95–108.
- Akhtar, S., Hughes, M. D., Khan, A., Bibby, M., Hussain, M., Nawaz, Q., Double, J., and Sayyed, P. (2000) *Adv. Drug Deliv. Rev.* 44, 3–21.
- Tari, A. M., and Lopez, B. G. (2001) *Curr. Opin. Invest. Drugs* 2, 1450–1453.
- Garcia, C. C., Seksek, O., Grzybowska, J., Borowski, E., and Bolard, J. (2000) *Pharmacol. Ther.* 87, 255–277.
- Dokka, S., and Rojanasakul, Y. (2000) *Adv. Drug Deliv. Rev.* 44, 35–49.
- Protozanova, E., and Macgregor, R. B., Jr. (1996) *Biochemistry* 35, 16638–16645.
- Poon, K., and Macgregor, R. B., Jr. (1998) *Biopolymers* 45, 427–434.
- Protozanova, E., Lawrence, K., and Macgregor, R. B., Jr. (1998) *Biopolymers* 49, 287–295.
- Protozanova, E., and Macgregor, R. B., Jr. (1998) *Biophys. J.* 75, 982–989.
- Protozanova, E., and Macgregor, R. B., Jr. (1998) *Biophys. Chem.* 75, 249–257.
- Protozanova, E., and Macgregor, R. B., Jr. (1999) *Electrophoresis* 20, 1950–1957.
- Poon, K., and Macgregor, R. B., Jr. (1999) *Biophys. Chem.* 79, 11–23.
- Protozanova, E., and Macgregor, R. B., Jr. (2000) *Biophys. Chem.* 84, 137–147.
- Poon, K., and Macgregor, R. B., Jr. (2000) *Biophys. Chem.* 84, 205–516.
- Protozanova, E., and Macgregor, R. B., Jr. (2001) *Biopolymers* 58, 355–358.
- Batalia, M. A., Protozanova, E., Macgregor, R. B., Jr., and Erie, D. A. (2002) *Nano Lett.* 2, 269–274.
- Wu-Pong, S. (2000) *Adv. Drug Deliv. Rev.* 44, 59–70.
- Diesbach, P., N'Kuli, F., Berens, C., Sonveaux, E., Monsigny, M., Roche, A. C., and Courtoy, P. J. (2002) *Nucleic Acids Res.* 30, 1512–1521.
- Diesbach, P., Berens, C., N'Kuli, F., Monsigny, M., Sonveaux, E., Wattiez, R., and Courtoy, P. J. (2000) *Nucleic Acids Res.* 28, 868–874.
- Deniset, F., and Lang, R. (1986) *J. Immunol. Methods* 89, 271–277.
- Timmons, S. R., Nwankwo, J. O., and Domann, F. E. (2002) *Oral Oncol.* 38, 281–290.
- Graham, J. (1984) in *Centrifugation: a practical approach* (Rickwood, D., Ed.) pp 161–182, IRL Press, Eynsham.
- Crooke, R. M. (1991) *Anti-Cancer Drug Des.* 6, 609–646.
- Zamecnik, P., Aghajanian, J., Zamecnik, M., Goodchild, J., and Witman, G. (1994) *Proc. Natl. Acad. Sci. U.S.A.* 91, 3156–3160.
- Beltinger, C., Saragovi, H. U., Smith, R. M., LeSauter, L., Shah, M., DeDionisio, L., Christensen, L., Raible, A., Jarett, L., and Gewirtz, A. M. (1995) *J. Clin. Invest.* 95, 1814–1823.
- Shoji, Y., Akhtar, S., Periasamy, A., Herman, B., and Juliano, R. L. (1991) *Nucleic Acids Res.* 19, 5543–5550.
- Boiziau, C., and Toulme, J. J. (1991) *Biochimie* 73, 1403–1408.
- Hawley, P., and Gibson, I. (1996) *Antisense Nucleic Acid Drug Dev.* 6, 185–195.
- Corrias, S., and Cheng, Y. C. (1998) *Biochem. Pharmacol.* 55, 1221–1227.
- Bennett, R. M., Hefeneider, S. H., Bakke, A., Merritt, M., Smith, C. A., Mourich, D., and Heinrich, M. L. (1988) *J. Immunol.* 140, 2937–2972.
- Silverstein, S. C., Steinman, R. M., and Cohn, Z. A. (1977) *Annu. Rev. Biochem.* 46, 669–722.
- Slapak, C. A., Lecerf, J. M., Daniel, J. C., and Levy, S. B. (1992) *J. Biol. Chem.* 267, 10638–10644.
- Pouton, C. W., Uduchi, A. N., Milroy, D. A., and Lucas, P. (1998) in *Self assembling complexes for genes delivery: From laboratory to clinical trial* (Kabanov, A. V., Felgner, P. L., and Seymour, L. W., Eds.) pp 255–273, John Wiley & Sons, New York.
- Guvakova, M. A., Yakubov, L. A., Vlodavsky, I., Tonkinson, J. L., and Stein, C. A. (1995) *J. Biol. Chem.* 270, 2620–2627.
- Fennewald, S. M., and Rando, R. F. (1995) *J. Biol. Chem.* 270, 21718–21721.
- Benimetskaya, L., Loike, J. D., Khaled, Z., Loike, G., Silverstein, S. C., Cao, L., Khoury, J., Cai, T. Q., and Stein, C. A. (1997) *Nat. Med.* 3, 414–420.
- Suzuki, T., Futaki, S., Niwa, M., Tanaka, S., Ueda, K., and Sugiura, Y., (2002) *J. Biol. Chem.* 277, 2437–2443.
- Bennet, R. M., Gabor, G. T., and Merritt, M. M. (1985) *J. Clin. Invest.* 76, 2182–2190.
- Loke, S. L., Stein, C. A., Zhang, X. H., Mori, K., Nakanishi, M., Subasinghe, C., Cohen, J. S., and Neckers, L. M. (1989) *Proc. Natl. Acad. Sci. U.S.A.* 86, 3474–3478.

40. Yakubov, L. A., Deeva, E. A., Zarytova, V. F., Ivanova, E. M., Ryte, A. S., Yurchenko, L. V., and Vlassov, V. V. (1989) *Proc. Natl. Acad. Sci. U.S.A.* 86, 6454–6458.
41. Hefeneider, S. H., Bennett, R. M., Pham, T. Q., Cornell, K., McCoy, S. L., and Heinrich, M. C. (1990) *J. Invest. Dermatol.* 94, 79S–84S.
42. Akhtar, S., Basu, S., Wickstrom, E., and Juliano, R. L. (1991) *Nucleic Acids Res.* 19, 5551–5559.
43. Goodarzi, G., Watabe, M., and Watabe, K. (1991) *Biochem. Biophys. Res. Commun.* 181, 1343–1351.
44. Akhtar, S., Beck, G. F., Hawley, P., Irwin, W. J., and Gibson, I. (1996) *Antisense Nucleic Acid Drug Dev.* 6, 197–206.
45. Beltinger, C., Saragovi, H. U., Smith, R. M., LeSauter L., Shah, M., DeDionisio, L., Christensen, L., Raible, A., Jarett, L., and Gewirtz, A. M. (1995) *J. Clin. Invest.* 95, 1814–1823.
46. Ohkuma, S., and Poole, B. (1978) *Proc. Natl. Acad. Sci. U.S.A.* 75, 3327–3331.
47. Ginsburg, H., and Geary, T. G. (1987) *Biochem. Pharmacol.* 36, 1567–1576.
48. Tonkinson, J. L., Guvakova, M., Khaled, Z., Lee, J., Yakubov, L., Marshall, W. S., Caruthers, M. H., and Stein, C. A. (1994) *Antisense Res. Dev.* 4, 269–278.
49. Nakai, D., Seita, T., Terasakai, T., Iwasa, S., Shoji, Y., Mizushima, M., and Sugiyama, Y. (1996) *J. Pharmacol. Exp. Ther.* 278, 1362–1372.
50. Kock, J., Borst, E. V., and Schlicht, H. J. (1996) *J. Virol.* 70, 5827–5831.
51. Hawtrey, A., Joubert, D., van Jaarsveld, P., Pieterse, A., van Zyl, J., and Ariatti, M. (2002) *Drug Deliv.* 9, 47–53.
52. Stein, C. A., Tonkinson, J. L., Zhang, L. M., Yakubov, L., Gervasoni, J., Taub, R., and Rotenberg, S. A. (1993) *Biochemistry* 32, 4855–4861.
53. Zamecnik, P., Aghajanian, J., Zamecnik, M., Goodchild, J., and Witman, G. (1994) *Proc. Natl. Acad. Sci. U.S.A.* 91, 3156–3160.
54. Wu-Pong, S., Weiss, T. L., and Hunt, C. A. (1994) *Cell. Mol. Biol.* 40, 843–850.

BI034290I